

Iron-titanium oxide minerals of Cretaceous to Paleogene volcanic rocks in western Chugoku district, Southwest Japan

— Special reference to manganese content of ilmenites —

TERUYOSHI IMAOKA and KAZUO NAKASHIMA

*Institute of Geology and Mineralogy, Faculty of Science,
Hiroshima University, Hiroshima 730, Japan*

NOBUHIDE MURAKAMI

*Institute of Earth Sciences, Faculty of Liberal Arts,
Yamaguchi University, Yamaguchi 753, Japan*

Fe-Ti oxide minerals of Cretaceous to Paleogene volcanic rocks in the western Chugoku district, Southwest Japan, have been examined mineralogically by means of electron microprobe. The volcanic rocks are divided into the Cretaceous Kanmon, Shunan, Hikimi, Abu and Paleogene Tamagawa Groups. Magnetite predominates in the volcanic rocks of the Kanmon, some of the Shunan, and Tamagawa Groups, while it is generally absent in those of Hikimi and Abu Groups. Chromian spinel has been found from the basaltic andesites of the Kanmon and Tamagawa Groups. The magnetic susceptibility of whole rock well reflects the above-described difference of the magnetite content, that is, χ -value is higher than 50×10^{-6} emu/g for the Kanmon, some of the Shunan and Tamagawa Groups, while it is lower than that for the Hikimi and Abu Groups.

Ilmenite is contained in almost all volcanic rocks examined, and its mode of occurrence is classified into three main types; 1) independent type, 2) trellis type, 3) composite type. Manganese least concentrates in the independent type. The difference of the MnO content of ilmenite among the five volcanic groups is far larger than that of the mode of occurrence and it is well distinguished in the FeTiO_3 - Fe_2O_3 - MnTiO_3 triangular diagram. That is, ilmenites from the Paleogene Tamagawa volcanic rocks are higher in MnTiO_3 and Fe_2O_3 molecules than those of the Cretaceous volcanic rocks (e.g., Kanmon, Hikimi and Abu Groups). Ilmenites from the Shunan Group are intermediate between the above-cited two groups of composition. In general, ilmenites from Paleogene volcanic rocks are richer in MnTiO_3 and Fe_2O_3 molecules than Cretaceous ones. Similar tendency in respect to age is observed in ilmenites of plutonic rocks, too. The $\text{Mn}^{2+}/\text{Fe}^{2+}$ ratio of ilmenite depends on temperature, Mn/Fe ratio of source magma and f_{O_2} . Available data indicate that high Mn-concentration in ilmenites from Paleogene igneous rocks may be attributable to high f_{O_2} during the formation of ilmenite.

Introduction

As is known well, the Japanese Islands are one of the sites of violent felsic igneous activity in the Circum-Pacific region during the Mesozoic to early Tertiary age. In the

Inner Zone of Southwest Japan, the igneous rocks related to this activity are distributed broadly and are divided into several cycles, illustrating typical volcano-plutonic association. However, the mutual petrologic correspondence and/or genetic

relationship among the component rocks within the same cycle of activity have not been fully clarified.

In recent years, remarkable data such as isotope age, whole rock and constituent mineral chemistry, magnetic susceptibility, stable isotope ratio and so on, have been accumulated concerning the Cretaceous to Paleogene granitoids in Japan, but the data are scarce on the volcanic rocks closely associated with these plutonic rocks, which have been investigated only geologically and stratigraphically. In western Chugoku, however, our recent investigation leads to the interesting conclusion on the late Mesozoic to early Tertiary volcanic rocks (Imaoka and Murakami, 1979; Murakami and Imaoka, 1980; Imaoka and Nakashima, in prep.), especially on the constituent oxide minerals, assemblage and chemistry of which are clearly discernible in each of the volcanic formations.

The opaque mineral oxides form a small but ubiquitous constituent of all igneous rocks, and are an important mineral group from the standpoint of their yielding data on geothermometry and oxygen geobarometry (Haggerty, 1976). In this paper, we report the optical and electron microprobe studies of these Fe-Ti oxide minerals of

volcanic rocks with special reference to the MnO content of ilmenite.

Geological setting

According to Murakami (1974), the late Mesozoic to early Tertiary volcanic formations of the title area are classified into five Groups, Kanmon, Shunan, Hikimi, Abu and Tamagawa, in ascending order as shown in Table 1. The geology of these volcanic formations* is briefly outlined below. Major elements analyses and magnetic susceptibility of 51 whole rock specimens used for the analysis of oxide minerals are listed in Table 2.

The lower to middle Cretaceous Kanmon Group is divided into the lower Wakino Subgroup and the upper Shimonoseki Subgroup (Hase, 1958). The volcanism of this group was initiated by small-scale felsic volcanism as indicated by tuffite or tuffaceous sediments in the Wakino Subgroup. The volcanism became more prominent in the Shimonoseki Subgroup, which consists mainly of a large volume of basaltic andesite to andesite lava and pyroclastic rocks with minor amounts of dacitic to rhyolitic pyroclastic rocks.

The Shunan Group unconformably overlies the Kanmon Group and shows

Table 1. Stratigraphy and major component volcanic rocks of the western Chugoku district, Southwest Japan

AGE	GROUP	MAJOR COMPONENT VOLCANIC ROCKS	SiO ₂ (wt.%)
PALEO-GENE	Tamagawa	rhyodacite-dacite(pyroclastic rocks) > andesite-basaltic andesite(lava & pyroclastic rocks) > rhyolite(lava & pyroclastic rocks)	50.5-74.6
	Abu	rhyolite-rhyodacite(pyroclastic rocks) >> andesite(lava & pyroclastic rocks)	55.4-77.9
CRETACEOUS	Hikimi	rhyolite-dacite(pyroclastic rocks)	65.4-77.5
	Shunan	dacite-andesite(lava & pyroclastic rocks) > rhyolite-rhyodacite(pyroclastic rocks)	56.1-76.1
	Kanmon	andesite-basaltic andesite(lava & pyroclastic rocks) >> rhyolite-dacite(pyroclastic rocks)	50.0-72.6

* No details of the petrography or chemistry are given here, so the reader is requested to refer to the original papers (Imaoka and Murakami, 1979; Murakami and Imaoka, 1980).

Table 2. Chemical analyses and magnetic susceptibility of volcanic rocks containing analyzed oxide minerals

Sp. No. ^a	1	2	3*	4	5	6	7	8	9	10	11	12*	13*	14	15	16	17
SiO ₂	52.02	52.66	55.86	56.04	57.62	59.20	61.46	64.20	70.02	53.92	57.35	59.65	60.23	63.73	57.10	59.91	65.44
TiO ₂	1.09	0.90	0.91	0.68	0.65	0.82	0.60	0.38	0.28	0.94	0.89	1.00	0.88	0.54	0.66	1.07	0.45
Al ₂ O ₃	15.79	16.31	17.47	17.63	17.17	14.79	16.53	15.96	16.37	17.28	17.21	18.01	16.95	15.81	16.99	16.78	16.29
Fe ₂ O ₃	1.43	4.13	2.07	3.49	1.81	1.50	0.91	2.63	0.97	0.46	1.47	1.84	0.24	2.42	0.51	0.70	1.13
FeO	6.71	4.37	4.40	3.85	4.49	5.75	4.05	2.19	0.65	7.73	4.91	4.25	3.87	2.34	6.38	6.49	3.96
MnO	0.11	0.12	0.15	0.04	0.05	0.13	0.01	0.05	0.02	0.29	0.12	0.13	0.14	0.10	0.17	0.28	0.12
MgO	6.12	5.34	3.60	3.65	3.07	4.96	2.58	1.75	1.05	4.79	3.38	2.25	2.84	2.00	3.69	3.46	1.18
CaO	10.55	8.27	6.73	7.10	5.02	5.54	5.73	3.62	1.59	9.66	6.52	6.86	6.71	4.50	8.01	6.96	3.04
Na ₂ O	3.71	3.46	2.58	2.86	5.26	3.56	4.12	4.09	5.23	2.32	2.86	3.09	3.02	2.63	2.95	2.12	3.50
K ₂ O	1.05	2.58	1.34	0.46	2.95	1.57	2.47	3.63	2.05	0.81	2.56	2.28	2.40	3.13	1.58	1.57	3.14
H ₂ O(+)	0.90	0.86	4.17	3.46	1.31	1.28	1.07	0.94	1.71	1.73	2.13	0.48	2.35	2.66	1.60	0.77	0.89
H ₂ O(-)	0.28	0.40	0.72	0.30	0.16	0.21	0.21	0.16	0.24	0.07	0.40	0.16	0.37	0.05	0.06	0.11	0.21
P ₂ O ₅	0.12	0.06	n.d.	0.12	0.13	0.18	0.06	0.02	0.03	0.06	n.d.	n.d.	n.d.	0.19	0.10	n.d.	0.21
Total	99.88	99.46	100.00	99.68	99.69	99.49	99.80	99.62	100.21	100.06	99.80	100.00	100.00	100.10	99.80	100.22	99.56
χ^b	5260	4240	410	1030	354	562	29	1290	20	27	22	564	17	59	51	402	n.d.
Reference ^c	3	3	3	1	2	3	3	2	2	3	1	3	3	3	1	3	1

Sp. No. ^a	18	19	20	21	22	23	24	25	26	27*	28	29	30	31	32	33	34
SiO ₂	66.24	66.25	66.30	66.39	67.19	67.32	68.30	68.31	69.53	71.15	74.20	74.66	75.56	75.93	55.43	68.64	70.26
TiO ₂	0.15	0.43	0.67	0.23	0.65	0.41	0.38	0.45	0.33	0.39	0.20	0.17	0.03	0.01	0.77	0.30	0.23
Al ₂ O ₃	16.26	15.54	15.71	16.21	15.61	15.67	14.87	15.21	14.84	14.39	13.32	12.62	13.41	12.18	16.94	14.55	14.61
Fe ₂ O ₃	1.14	1.21	1.26	1.13	1.25	0.67	0.42	1.69	0.30	0.31	0.18	0.43	0.07	0.84	4.08	2.24	1.78
FeO	3.36	2.73	3.21	3.43	2.53	3.37	3.47	3.17	2.52	2.96	1.84	1.86	0.29	0.72	3.56	1.05	0.74
MnO	0.08	0.19	0.08	0.08	0.01	0.06	0.06	0.08	0.09	0.12	0.08	0.05	0.03	0.03	0.16	0.09	0.10
MgO	0.94	0.91	1.11	0.60	0.97	0.98	0.97	0.96	0.43	0.74	0.54	0.24	0.09	0.07	3.79	0.34	0.40
CaO	2.56	4.04	2.63	3.18	3.58	3.10	1.70	3.18	2.54	2.83	1.40	1.43	1.39	0.95	5.97	3.07	2.83
Na ₂ O	4.33	3.47	3.72	3.98	3.71	3.56	4.07	3.72	3.20	3.55	3.77	3.50	3.61	3.61	4.25	2.56	4.25
K ₂ O	3.14	3.74	2.95	3.02	2.95	3.36	3.78	3.00	4.59	3.31	3.73	4.34	4.20	3.76	1.10	4.67	4.13
H ₂ O(+)	0.89	0.82	1.58	0.76	1.02	0.82	1.28	0.53	0.87	0.19	0.51	0.73	0.58	1.63	2.70	2.26	0.42
H ₂ O(-)	0.25	0.09	0.23	0.27	0.42	0.07	0.20	0.07	0.07	0.06	0.07	0.20	0.05	0.34	0.66	0.22	0.19
P ₂ O ₅	0.18	n.d.	0.04	0.18	0.21	0.06	0.07	0.09	0.06	n.d.	0.02	0.02	0.01	0.01	0.06	0.08	0.05
Total	99.52	99.42	99.49	99.46	100.10	99.45	99.57	100.46	99.37	100.00	99.86	100.25	99.32	100.08	99.47	100.07	99.99
χ^b	21	37	n.d.	19	14	n.d.	24	n.d.	n.d.	22	n.d.	16	14	12	860	166	292
Reference ^c	1	1	1	2	1	1	1	1	1	3	1	2	2	2	1	2	2

Sp. No. ^a	35	36*	37*	38*	39*	40*	41	42	43	44	45	46	47	48	49	50	51
SiO ₂	73.35	66.23	68.31	71.42	72.93	73.24	54.01	54.61	55.45	56.22	58.23	58.59	60.00	66.87	69.28	71.03	73.82
TiO ₂	0.20	0.80	0.59	0.42	0.25	0.18	0.84	1.03	0.99	0.83	0.85	1.12	0.85	0.12	0.54	0.37	0.32
Al ₂ O ₃	13.65	14.32	14.81	15.21	13.58	14.01	18.31	19.21	17.59	16.66	16.52	17.78	16.99	15.83	16.48	15.17	14.80
Fe ₂ O ₃	0.86	0.51	0.30	0.25	0.87	0.39	3.69	4.43	1.72	2.02	3.71	2.76	3.29	2.19	1.43	1.52	1.03
FeO	1.58	4.87	3.95	2.59	1.40	1.70	2.81	2.47	5.15	4.97	2.90	3.76	1.99	1.59	1.58	1.69	1.61
MnO	0.03	0.19	0.14	0.07	0.10	0.10	0.09	0.21	0.22	0.16	0.11	0.19	0.15	0.12	0.13	0.14	0.11
MgO	0.53	2.04	1.42	0.54	0.35	0.44	4.28	2.91	4.56	5.33	2.35	2.35	2.44	1.50	0.88	0.71	0.49
CaO	1.55	4.25	3.57	3.64	1.79	2.04	7.07	4.67	7.93	8.43	3.73	4.34	4.13	3.53	2.16	1.96	2.04
Na ₂ O	2.86	2.95	3.02	2.80	3.51	3.17	4.29	3.38	3.46	2.89	4.72	4.17	4.22	2.99	3.42	3.04	3.29
K ₂ O	3.79	2.89	3.28	2.69	4.45	4.05	1.59	3.70	0.98	0.70	1.53	1.85	1.38	1.55	2.30	2.71	2.10
H ₂ O(+)	1.81	0.89	0.55	0.15	0.71	0.54	2.02	2.76	1.25	1.80	3.28	2.56	3.47	2.35	1.46	1.72	0.48
H ₂ O(-)	0.18	0.06	0.06	0.22	0.06	0.14	0.29	0.50	0.14	0.44	1.27	0.50	0.78	1.16	0.46	0.36	0.13
P ₂ O ₅	0.02	n.d.	n.d.	n.d.	n.d.	n.d.	0.25	n.d.	n.d.	n.d.	0.21	n.d.	n.d.	0.11	n.d.	n.d.	n.d.
Total	100.41	100.00	100.00	100.00	100.00	100.00	99.54	99.88	99.44	100.45	99.41	99.97	99.69	99.91	100.12	100.42	100.22
χ^b	20	20	12	68	9	14	n.d.	944	766	260	350	1350	270	n.d.	82	26	255
Reference ^c	2	3	3	3	3	3	1	3	3	3	1	3	3	1	3	3	3

Nos. 1–9: Kanmon Group, Nos. 10–16: Shunan Group and its correlatable formation (Nos. 15, 16: Kisa Group), Nos. 17–31: Hikimi Group. Nos. 32–40: Abu Group and its correlatable formation (Nos. 36–40: Takada Rhyolite), Nos. 41–51: Tamagawa Group.

^a Specimen numbers with star indicate that they are analyzed by the direct fusion method described by Suzuki *et al.* (1977) and are recalculated to make the total of 12 major oxides 100%.

^b Magnetic susceptibility ($\times 10^{-6}$ emu/g).

^c 1: Imaoka and Murakami (1979), 2: Murakami and Imaoka (1980), 3: This study.

Analysts: T. Imaoka (Nos. 3, 11, 19, 27, 36–40, 42–51),

K. Nakashima (Nos. 10, 12, 13) and Murakami (others).

sporadic distribution extending in an E-W direction. The volcanic rocks of this group consist of andesitic lava and pyroclastic rocks, dacitic to rhyodacitic pyroclastic rocks and dacitic to rhyodacitic intrusive breccia. The intrusive breccia was considered in intimate connection with the formation of the cauldron structure (Murakami and Matsusato, 1970). The Kisa andesite formation (Yoshida, 1961) in the central Chugoku district is correlatable to the Shunan Group.

The Hikimi Group is developed extending about 100 km or more with 20–40 km width in the Chugoku mountainland. According to Murakami (1974), the contacts of this group with basement rocks (upper Paleozoic and Sangun metamorphic rocks) are tectonic lines dipping almost vertically. Consequently, a large graben-like structure with E-W to NE-SW axis is suggested for this group. A large part of this group is composed of dacitic to rhyolitic ignimbrite.

The Abu Group overlies the Shunan Group unconformably. It consists essentially of rhyolitic to rhyodacitic welded tuff intercalated with thin tuffaceous sediments of lacustrine origin. Dacitic to andesitic rocks are also interbedded in the lower and upper horizons. The total thickness is summed up to 2000 to 2500 m or more. The distribution of this group is confined to the area extending from the Chugoku mountainland to the San'in district. The mode of emplacement of these volcanic rocks has not been ascertained, although there are some evidences possibly suggesting a large-scale collapse comparable to the volcano-tectonic depression proposed by Williams (1941), as deduced from the long-continued fault breccia zone along the contact with basement rocks.

The Takada rhyolite in the central Chugoku district unconformably covers the Kisa andesite (Yoshida, 1961). It consists mainly of rhyolitic to dacitic welded tuff. According to the writers' preliminary investigation, the Takada rhyolite most resembles to the Abu Group in regard to the lithofacies, whole rock and constituent mineral chemistry and magnetic susceptibility.

The Paleogene Tamagawa Group and its correlatives are distributed in the western San'in district. The volcanic rocks of them occur in intimate association with gabbroic to granitic rocks, forming the volcano-plutonic complexes. Their distribution shows a roughly linear arrangement, with an interval of about 20 km, parallel to the Japan Sea. They are named Tamagawa, Masuda, Hamada, Haza, Sakurae and Kawamoto complexes from west to east. Almost all of these complexes are considered to form the cauldron structure (Murakami, 1973; Matsuda, 1976; Imaoka, 1978 MS; Nakamura, 1979; Masuda Research Group, 1982; Murakami *et al.*, 1982). The component volcanic rocks are andesitic to rhyolitic pyroclastic rocks and lava, with a small amount of lacustrine sediments intercalated in the lower horizon.

Mode of occurrence of Fe-Ti oxide minerals

Polished thin sections of about 200 specimens were observed under the ore microscope. The results are given below.

1. Kanmon Group

The volcanic rocks of this group have generally suffered strong alteration. Consequently, only the least altered samples are provided for detailed petrographic studies. In the samples examined, magnet-

ite*, not ilmenite, is a dominant opaque mineral regardless of the rock type and stratigraphic position of rocks.

a) Andesitic rocks

In the basaltic andesite to andesite lava, magnetite occurs as phenocryst and also as a groundmass mineral (Fig. 1, no. 1), varying between 0.3 and 5% in volume. Phenocrystic magnetite is subhedral to anhedral and has commonly oriented lamellae of ilmenite, a few to several tens of microns wide along its (111) plane. It rarely occurs as homogeneous single grains. In sample no. 5, magnetite shows granule intergrowth with ilmenite. In some cases, magnetite is corroded and often martitized along the cracks and/or periphery. Maximum grain size of phenocrystic magnetite attains to about 1 mm, but a few hundred microns are the commonest size. There is no occurrence of phenocrystic ilmenite except sample no. 3. In the groundmass, magnetite and ilmenite occur usually as euhedral to subhedral grains of a few to several tens of microns in diameter. The minimum ratio of magnetite to magnetite+ilmenite is 0.3.

It must be stressed that basaltic andesite contains chromian spinel. In andesite lava, it is present as phenocryst of 200–400 microns in size, while in andesite tuff, it occurs as euhedral to subhedral grain up to 50 microns in the matrix. All of these chromian spinels show a distinct zoning with the dark grayish brown core and the light brown rim.

b) Dacitic to rhyolitic rocks

In the dacite to rhyolite pyroclastic rocks, magnetite is the dominant opaque accessory mineral amounting to 0.2 to 1.5% by volume. It is present as euhedral to

subhedral phenocrystic grains of a few hundred microns, often one thousand microns. Ilmenite lamellae of several microns wide, often up to several tens of microns, are characteristic of the magnetite. No phenocrystic ilmenite is observed. In the matrix, magnetite and ilmenite occur as subhedral discrete grains which are often altered to maghemite and hematite+rutile, respectively. Secondary minute ilmenite associated with chloritization of biotite is also observed.

2. *Shunan Group*

Microscopically, the volcanic rocks of this group can be divided into two distinct types on the basis of the relative modal abundance of opaque minerals, magnetite-predominant type and ilmenite-predominant type. These two types have no discernible difference in the stratigraphic position, rock type, silicate mineral assemblage and texture of the rocks.

a) Andesite lava

In the magnetite-predominant type, phenocrystic magnetite is present as euhedral to subhedral grains of two hundred to one thousand microns in diameter. Euhedral magnetite of about one hundred microns has been observed also in the groundmass. In this type, ilmenite occurs generally as lamellae and/or granule intergrowth within the magnetite and as euhedral single grain in the groundmass. In the ilmenite-predominant type, ilmenite occurs as subhedral to anhedral phenocrystic single grain. This mineral has a maximum size of seven hundred microns. It is often corroded. Euhedral ilmenite, less than one hundred microns in size, is also present in the groundmass. In this type, a small

* The term "magnetite" and "ilmenite" are used for convenience in place of magnetite-ulvöspinel series and ilmenite-hematite series, respectively.

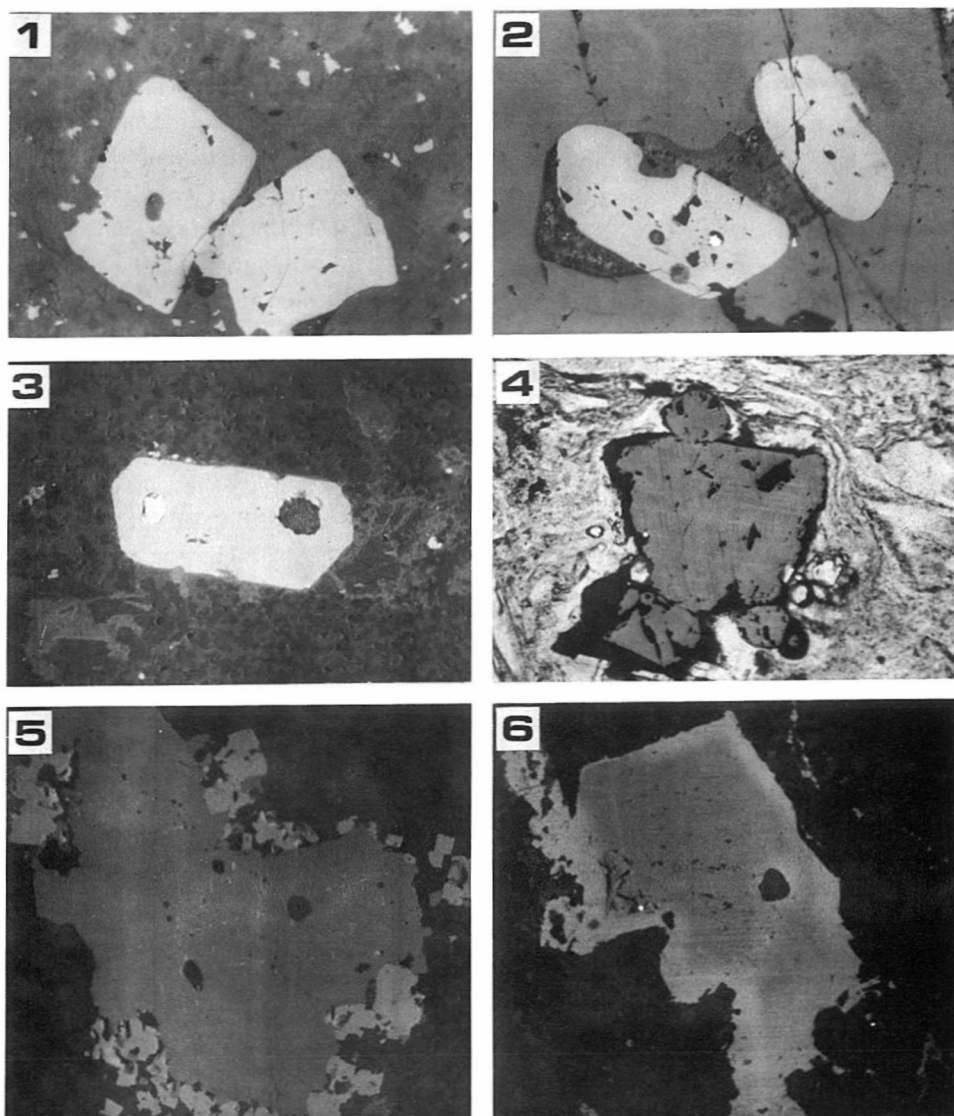


Fig. 1. Photomicrographs of Fe-Ti oxide minerals.
 no. 1: 0.43×0.30 mm, euhedral magnetite phenocryst (Usp. 45–50 mol. %) and groundmass magnetite (Usp. 76 mol. %) in andesite lava from the Kanmon Group (Sp. no. 4), no. 2: 1.09×0.76 mm, corroded ilmenite inclusion (independent grain type) in clinopyroxene andesite tuff from the Shunan Group (Sp. no. 11), no. 3: 0.33×0.23 mm, euhedral ilmenite phenocryst (independent grain type) having pyrrhotite inclusion in dacite tuff from the Hikimi Group (Sp. no. 17), no. 4: 0.43×0.30 mm, magnetite phenocryst having thin ilmenite lamellae in rhyolite welded tuff from the Paleogene Masuda cauldron, Tamagawa Group (Sp. no. 51), no. 5: 0.33×0.29 mm, ilmenite-magnetite composite grain in recrystallized rhyolite crystal tuff (Takada rhyolite). Euhedral magnetite (Usp. 3.5 mol. %) probably formed by recrystallization fringes the ilmenite phenocryst (Sp. no. 39), No. 6: 0.33×0.29 mm, zoned chromian spinel in basaltic andesite lava from Paleogene Hamada cauldron, Tamagawa Group (Sp. no. 7865–11).

amount of magnetite is observed in the groundmass and altered mafic minerals.

b) Dacitic to rhyodacitic pyroclastic rocks

In the magnetite-predominant type, magnetite occurs as homogeneous single grain in the dacitic rocks, but it shows the trellis intergrowth of thin ilmenite lamellae set in (111) plane in the rhyodacitic rocks. It is anhedral with maximum grain size of four hundred microns in the phenocryst but in the groundmass it is subhedral and is several tens of microns to hundred microns in length. In the ilmenite-predominant type, ilmenite is present as subhedral to anhedral phenocryst and single subhedral grain in the matrix. Some of this type contain no magnetite (e.g., nos. 10 and 13).

3. *Hikimi Group*

Volcanic rocks of this group are characterized by the virtual absence of magnetite. Ilmenite is the sole oxide mineral occurring as discrete subhedral to anhedral grains, sometimes euhedral with an optically homogeneous appearance (Fig. 1, no. 3). Modally it is 0.2–0.5% in volume in dacitic to rhyodacitic pyroclastic rocks, while less than 0.05% in rhyolitic pyroclastic rocks. Its grain size is commonly 20–100 microns, attaining to 600 microns in maximum. It is commonly corroded and more or less rounded in shape. In most cases, ilmenite is intimately associated with biotite, i.e., it is enclosed in the biotite and/or partly or completely fringed by the aggregate of euhedral biotite (5–70 microns) probably formed by recrystallization. It is also observed as small anhedral granules (20–30 microns) along the cleavage or periphery of biotite. Some of the ilmenite grains are armored by sphene, but they are generally

quite fresh.

The common presence of pyrrhotite is another conspicuous feature of the volcanic rocks of this group. Its mode is less than 0.1% in volume. In many cases, it is enclosed in ilmenite. It occurs also in the shell part of plagioclase and along the periphery of biotite. It is usually anhedral and is 40–80 microns in size, attaining to a few hundred microns in rare cases.

4. *Abu Group*

Volcanic rocks of this group are distinguished by extremely small amounts of Fe-Ti oxide minerals (0.02–0.4 volume %) dominated by ilmenite. Excepting some specimens, magnetite is entirely absent and ilmenite is the sole oxide phase. In exceptional samples, euhedral magnetite of 10 to 20 microns in size, is set in the matrix. Moreover, many minute grains of anhedral magnetite are observed within the chlorite altered from biotite. In these samples, magnetite is not observed as phenocrysts, and ilmenite predominates over magnetite in volume. Ilmenite is found in phenocrysts as well as in the matrix. Phenocrystic ilmenite is euhedral to subhedral, and its common grain size ranges from 300 to 500 microns. Ilmenite in the matrix shows a subhedral to anhedral form, varying from 5 to 50 microns in diameter. Occasionally it is included poikilitically in plagioclase. It occurs also as a secondary mineral associated with chloritization of biotite. Rutile and hematite are often observed as an oxidation product of ilmenite. Sphenization of ilmenite is common, and this proceeds along the grain boundary of ilmenite to form the large mass of sphene including small remnants of ilmenite.

Various kinds of sulfide minerals*

* Lacking pyrrhotite

such as pyrite, chalcopyrite, sphalerite and covellite occur commonly along cracks as secondary hydrothermal veins or disseminated particles.

5. Tamagawa Group

Although the volcanic rocks of this group have a wide range of chemical composition from basaltic andesite to rhyolite, there is no great difference in constituent opaque minerals; that is, magnetite predominates over ilmenite in all of the rock types without exception.

a) Andesitic rocks

In andesite lava, magnetite constitutes 0.3 to 1.5% in volume, whereas ilmenite is up to 0.1%, even absent in some specimens (nos. 41 and 45). The volume ratio of ilmenite to ilmenite+magnetite ranges from 0 to 0.15.

Magnetite occurs as phenocrysts and also as a groundmass mineral. Phenocrystic magnetite is euhedral to anhedral. The range of grain size is commonly 100 to 200 microns, attaining to a maximum value of 600 microns. Some of the magnetite contain three sets of ilmenite lamellae of a few to ten microns wide along (111) plane. These lamellae are frequently concentrated along cracks, around silicate inclusions and most significantly along magnetite grain boundary. Groundmass magnetite occurs as minute grains of about 10 microns. Its peripheral part is often altered to maghemite.

Ilmenite occurs commonly in the groundmass as anhedral single grains of 10 to 100 microns in size. It is present also as a phenocrystic mineral in a few cases, when they are euhedral crystals up to about 200 microns. In relation to magnetite, it occurs as lamellae described above and as composite grains (Fig. 2), and far less frequently as granules of ilmenite "exsolved" outside

the borders of magnetite.

In andesitic to basaltic andesite lava from the Hamada and Masuda cauldrons, chromian spinel has been found in some specimens. It occurs as tiny anhedral to subhedral inclusions in olivine pseudomorphs and also as independent microphenocrysts in the groundmass. It shows a conspicuous zoning with the dark-gray core surrounded by the rim of low reflectivity (Fig. 1, no. 6). In these specimens, chrome-rich magnetite coexists as strings or trains of grains outlining olivine pseudomorphs.

b) Dacitic to rhyodacitic rocks

In the dacitic to rhyodacitic rocks, magnetite constitutes 0.05 to 0.6% in volume of rock, occurring as subhedral single grains up to 1000 microns and/or rarely as composite grains with ilmenite. It is often corroded and more or less rounded in shape. Some of the phenocrystic magnetites are fragmental in shape similar to the fragments of quartz and plagioclase. Frequently it has the fine sets of ilmenite lamellae in rhyolitic tuff (Fig. 1, no. 4). Ilmenite occurs as corroded single grains besides intergrowth with magnetite, and constitutes 0.1 to 0.5% in volume of rock. The volume ratio of ilmenite to ilmenite+magnetite is somewhat higher than that of andesite lava, being 0.2 to 0.7, commonly 0.2 to 0.3.

Sphenization of ilmenite and magnetite is pervasive in the rocks investigated. This may suggest the reaction of Fe-Ti oxides with a residual hydrothermal solution.

Sulfides are less abundant than Fe-Ti oxides. The commonest are pyrite and chalcopyrite, while pyrrotite, sphalerite and galena are found only occasionally. They occur as veins and/or disseminated particles. Petrological and stable isotopic data indicate that these sulfides are the products of intense geothermal activity

which occurred at a high-temperature hydrothermal stage subsequent to a magmatic stage (Imaoka *et al.*, 1977; Matsuhisa *et al.*, 1980).

Magnetic susceptibility of rock

Magnetic susceptibility was measured on powdered samples obtained from Cretaceous to Paleogene volcanic rocks in western Chugoku. The details of the results together with data on associated plutonic rocks are given in Imaoka and Nakashima (in prep.), who clarified the systematic variation of magnetic susceptibility in time and space.

Fig. 2 illustrates the relationship between the magnetic susceptibility and the SiO_2 content (wt. %) of volcanic rocks. The magnetic susceptibility of them ranges from 0 to 6000×10^{-6} emu/g. The rocks of each group provides a characteristic distribution range of the magnetic suscepti-

bility. The volcanic rocks of the Kanmon (50–65% SiO_2) and Tamagawa (50–75% SiO_2) Groups have generally high χ -values of 50 to 6000×10^{-6} emu/g and largely belong to the magnetite-series, whereas those of the Hikimi (65–78% SiO_2) and Abu (55–78% SiO_2) fall largely below 50×10^{-6} emu/g and belong to the ilmenite-series. In the volcanic rocks of the Shunan Group, the magnetic susceptibility ($10\text{--}400 \times 10^{-6}$ emu/g) is assigned to both the ilmenite-series and magnetite-series.

The magnetic susceptibility of rock is directly proportional to the volume percent of magnetite in the rock (e.g., Ishihara, 1979). Thus, the general decreasing tendency of magnetic susceptibility of the magnetite-series volcanic rocks, as the silica content increases, may reflect the gradual decrease of the magnetite content. These results of the magnetic susceptibility are in good agreement with those of the microscopic observa-

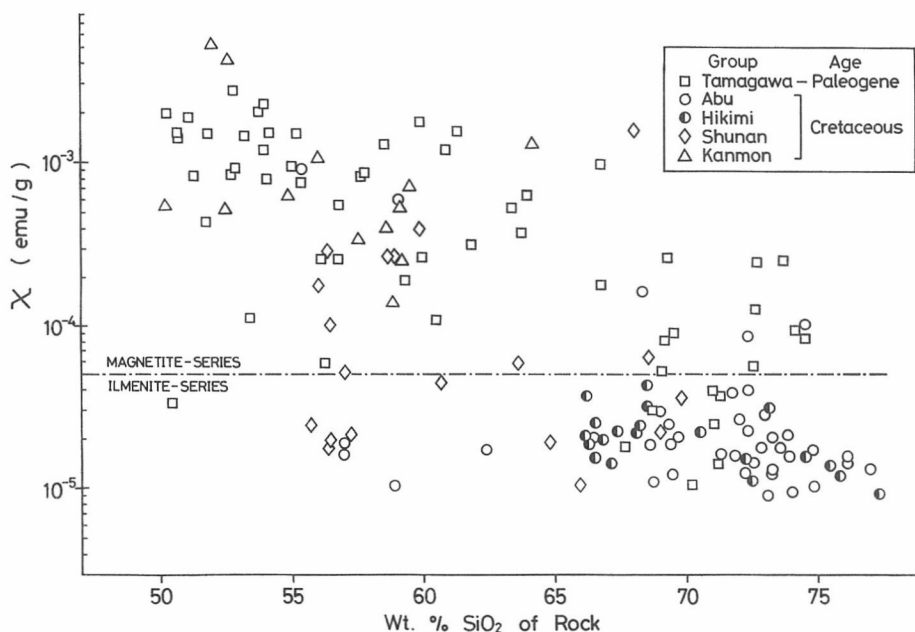


Fig. 2. Relationship between magnetic susceptibility and SiO_2 (wt. %) content of volcanic rocks.

tion in that a fairly large amount of magnetite is contained in the volcanic rocks of the Kanmon and Tamagawa Groups, while magnetite is generally absent in those of the Hikimi and Abu Groups in ordinary magnification.

Chemistry of Fe-Ti oxide minerals

Analytical procedure

Oxide minerals of 51 representative specimens from each of the groups were analysed with JXA-5A electron microprobe analyzer with 40° take-off angles at Hiroshima University. Instrument conditions

Table 3. Electron microprobe analyses of ilmenites

No ^a	1-1-1	1-1-2	1-2-3	2-1-1	2-1-2	2-2-3	3-1-7	3-2-9	5-1-5	6-1-1	6-2-2	7-1-1	7-2-2	9-1-1	10-1-1	10-1-2	11-1-3	11-1-4	12-1-7	12-2-2	
Occurrence ^b	G-I-C	G-I-R	G-I-C	G-I-C	G-I-R	G-I-C	P-I-C	P-I-C	P-C-I	G-I-C	G-I-C	G-I-C	G-I-C	G-I-C	P-I-C	P-I-R	P-I-C	P-I-R	P-I-R	P-I-R	P-L
SiO ₂	0.10	0.08	0.10	0.30	0.36	0.14	0.34	0.11	0.32	0.18	0.11	0.09	0.17	0.24	0.07	0.10	-	0.01	0.04	0.11	
TiO ₂	49.1	49.2	49.3	48.5	48.5	48.7	49.6	47.3	48.6	51.4	52.0	50.2	50.9	49.0	51.1	50.2	48.2	47.0	48.4	49.3	
Al ₂ O ₃	0.01	0.02	0.01	0.04	0.03	0.03	0.25	0.08	0.12	0.06	0.03	0.05	0.18	0.02	0.05	0.05	0.04	0.13	0.04	0.06	
Cr ₂ O ₃	0.03	0.03	0.02	0.05	0.04	0.03	0.08	0.08	0.12	0.05	0.03	0.04	0.04	0.03	0.08	0.11	0.08	0.09	0.06	0.03	
FeO ^c	45.0	44.9	46.2	46.5	46.3	46.5	46.4	49.5	46.4	42.4	41.7	42.5	41.5	48.9	43.6	42.9	48.2	49.3	46.8	44.7	
MnO	5.34	5.38	3.59	2.50	2.72	3.75	1.24	1.02	2.85	5.17	5.35	5.34	6.11	1.30	4.97	5.12	1.28	2.12	3.65	4.39	
MgO	0.21	0.10	0.13	0.77	0.54	0.50	1.13	0.09	0.08	0.07	0.10	0.09	0.09	0.02	0.12	0.12	1.28	0.07	0.12	0.11	
CaO	0.16	0.27	0.22	0.31	0.35	0.29	0.02	-	0.18	0.34	0.33	0.35	0.26	0.06	0.04	0.16	0.02	0.14	0.10	0.04	
Total	100.0	100.0	99.6	99.0	98.8	99.9	99.1	98.2	98.7	99.8	99.7	98.7	99.3	99.6	100.0	98.8	99.1	98.9	99.2	98.7	
Calculated normative components																					
MnTiO ₃	11.4	11.5	7.64	5.31	5.78	7.97	2.64	2.16	6.05	11.0	11.4	11.4	13.0	2.76	10.6	10.9	2.73	4.51	7.76	9.33	
FeTiO ₃	81.0	81.6	85.4	83.9	84.4	82.5	87.3	87.2	85.9	86.0	86.9	83.6	83.4	90.3	86.0	84.0	84.0	84.4	83.6	83.7	
Fe ₂ O ₃	7.40	7.01	6.44	7.57	7.07	8.31	5.61	9.11	6.34	1.86	0.93	3.21	2.25	6.83	3.26	3.46	9.34	10.3	7.95	5.65	
MgTiO ₃	0.63	0.30	0.40	2.31	1.60	1.50	3.37	0.27	0.24	0.51	0.31	0.27	0.26	0.06	0.36	0.36	3.83	0.20	0.35	0.34	
Total R ₂ O ₃	100.5	100.5	99.9	99.2	98.9	100.3	99.3	98.9	98.8	99.5	99.6	98.6	99.1	100.0	100.4	98.9	100.0	99.6	99.8	99.1	

No ^a	12-3-4	12-3-5	13-1-7	13-1-8	13-2-9	13-2-0	14-1-5	14-2-3	15-1-7	15-1-8	15-2-5	16-1-1	16-1-2	17-1-1	17-1-2	17-2-3	17-2-5	18-1-4	18-2-6	19-1-1
Occurrence ^b	P-I-C	P-I-R	P-I-C	P-I-R	P-I-C	P-I-R	P-I-C	P-I-C	P-I-C	P-I-R	P-I-C	P-I-C	P-I-R	P-I-C	P-I-R	P-I-C	P-I-R	P-I-C	P-I-C	P-I-C
SiO ₂	0.04	0.05	0.03	-	0.03	0.05	0.05	0.02	0.14	0.21	0.10	0.21	0.22	0.19	0.16	0.09	0.09	0.14	0.07	0.13
TiO ₂	48.0	49.4	49.0	47.2	48.9	48.3	48.1	48.1	50.5	50.4	51.7	48.8	49.3	49.9	50.6	51.0	51.2	49.4	49.6	49.5
Al ₂ O ₃	0.05	0.05	0.35	0.32	0.31	0.30	0.02	0.04	0.04	0.03	0.02	0.04	0.04	0.04	0.02	0.01	0.01	0.06	0.05	0.49
Cr ₂ O ₃	0.05	0.05	0.05	0.03	0.05	0.05	0.16	0.30	0.10	0.08	0.10	0.13	0.12	0.06	0.09	0.04	0.06	0.07	0.06	0.27
FeO ^c	44.9	43.4	47.2	46.8	46.3	46.8	46.6	46.5	43.1	43.0	42.6	46.2	45.9	47.1	46.7	46.0	45.7	47.7	47.3	47.2
MnO	5.56	5.68	1.88	2.61	2.53	3.46	3.22	3.41	4.78	4.87	5.36	3.66	3.71	2.84	2.97	3.16	3.22	2.58	3.17	0.88
MgO	0.08	0.07	1.59	0.66	0.79	0.19	0.09	0.13	0.29	0.28	0.19	0.15	0.10	0.09	0.05	0.05	0.06	0.05	0.04	0.08
CaO	0.05	0.05	0.03	0.07	0.07	0.09	0.19	0.08	0.02	0.09	0.06	0.02	0.01	0.01	0.02	0.01	0.04	0.01	0.03	0.06
Total	98.7	98.8	100.1	97.7	99.0	99.2	98.4	98.6	99.0	98.9	100.1	99.2	99.4	100.2	100.6	100.4	100.4	100.0	100.3	98.6
Calculated normative components																				
MnTiO ₃	11.8	12.1	3.99	5.55	5.39	7.36	6.85	7.25	10.2	10.4	11.40	7.77	7.90	6.04	6.31	6.72	6.84	5.49	6.75	1.87
FeTiO ₃	78.9	81.5	83.0	81.5	84.4	83.7	84.2	83.6	84.5	84.3	86.0	84.2	85.3	88.4	89.6	89.9	90.1	88.0	87.2	91.8
Fe ₂ O ₃	8.37	5.39	8.84	9.06	7.11	7.93	7.53	7.73	3.40	3.40	2.08	7.05	6.08	5.84	4.71	3.77	3.38	6.70	6.66	4.10
MgTiO ₃	0.25	0.20	4.74	1.96	2.35	0.57	0.28	0.39	0.88	0.84	0.57	0.45	0.31	0.26	0.14	0.15	0.18	0.16	0.12	0.23
Total R ₂ O ₃	99.4	99.3	101.0	98.4	99.6	99.9	99.0	99.3	99.1	99.1	100.2	99.6	99.8	100.6	100.9	100.6	100.6	100.5	100.9	98.8

No ^a	19-2-2	20-1-1	20-1-2	20-2-3	20-2-4	21-1-1	21-1-2	22-1-1	22-1-2	23-1-1	23-1-2	24-1-4	24-2-6	25-1-1	25-1-2	25-2-3	25-2-4	26-1-3	26-1-4	26-2-1
Occurrence ^b	P-I-C	P-I-C	P-I-R	P-I-C	P-I-R	P-I-C	P-I-R	P-I-C	P-I-R	P-I-C	P-I-R	P-I-C	P-I-C	P-I-C	P-I-C	P-I-C	P-I-R	P-I-C	P-I-R	P-I-C
SiO ₂	0.12	0.01	-	-	0.07	0.01	-	0.04	0.12	0.11	0.10	0.09	0.13	0.11	0.10	0.14	0.17	0.10	0.18	
TiO ₂	50.5	50.2	49.8	49.6	49.5	51.4	51.6	49.1	51.7	49.7	49.7	49.6	49.3	50.7	51.2	50.6	51.9	51.1	52.7	52.5
Al ₂ O ₃	0.04	0.12	0.07	0.05	0.06	0.03	0.03	0.02	0.03	0.04	0.03	0.03	0.04	0.03	0.06	0.03	0.05	0.04	0.04	0.03
Cr ₂ O ₃	0.07	0.09	0.10	0.08	0.07	0.05	0.05	0.04	0.05	0.05	0.07	0.06	0.06	0.06	0.08	0.07	0.07	0.05	0.08	0.03
FeO ^c	47.2	49.1	47.7	45.2	44.8	45.1	44.6	46.0	43.0	48.1	47.6	47.6	46.9	46.8	46.6	46.0	44.7	45.4	44.6	44.1
MnO	2.86	1.25	1.23	3.78	3.79	3.43	3.58	4.08	4.52	2.22	2.22	2.70	2.62	1.71	1.81	3.12	3.46	2.95	3.28	3.67
MgO	0.05	0.07	0.04	0.04	0.03	0.05	0.04	0.05	0.03	0.02	0.01	0.03	0.02	0.02	0.02	0.05	0.05	0.11	0.12	0.09
CaO	0.02	0.03	0.01	0.05	0.16	0.01	-	0.02	0.07	0.02	0.03	0.02	0.01	0.03	0.02	0.11	-	0.10	0.02	
Total	100.9	100.9	99.0	98.8	98.5	100.1	99.9	99.4	99.5	100.2	99.8	100.1	99.0	99.5	99.9	100.0	100.5	99.9	101.0	100.6
Calculated normative components																				
MnTiO ₃	6.08	2.65	2.63	8.03	8.06	7.29	7.62	8.69	9.61	4.72	4.73	5.74	5.58	3.63	3.85	6.63	7.35	6.27	6.97	7.81
FeTiO ₃	89.6	92.3	91.8	85.9	85.9	90.2	90.1	84.4	88.4	89.5	89.5	88.4	88.0	92.6	93.2	89.3	91.1	90.3	92.6	91.5
Fe ₂ O ₃	5.37	6.03	4.67	4.99	4.62	2.71	2.14	6.71	1.24	6.30	5.81	6.37	5.88	3.29	2.70	4.11	1.74	2.92	0.86	0.89
MgTiO ₃	0.14	0.21	0.13	0.11	0.10	0.15	0.13	0.16	0.13	0.06	0.04	0.10	0.05	0.06	0.06	0.15	0.15	0.32	0.37	0.26
Total R ₂ O ₃	101.3	101.4	99.4	99.2	98.8	100.4	100.1	100.0	99.5	100.7	100.2	100.7	99.6	99.7	99.9	100.3	100.4	99.9	100.9	100.5

No. ^a	27-1-1	27-1-2	28-1-1	28-2-2	29-1-1	30-1-1	30-1-2	31-1-1	31-1-2	32-1-3	32-2-5	32-3-6	33-1-1	34-1-1	34-2-2	34-3-3	34-4-4	35-1-1	36-1-6	36-2-7
Occurrence ^b	P-I-C	P-I-R	G-I-C	G-I-C	P-I-C	P-I-C	P-I-R	P-I-C	P-I-R	P-I-C	P-I-C	G-I-C	G-I-C	P-I-C	P-I-C	G-I-C	G-I-C	G-I-C	P-I-C	P-I-C
SiO ₂	0.09	0.09	0.11	0.10	0.04	0.03	0.04	0.17	0.19	-	-	0.05	0.07	-	0.04	0.06	0.02	0.26	0.12	0.09
TiO ₂	50.1	50.7	51.8	51.2	50.9	52.1	52.1	50.8	51.3	51.9	52.4	52.1	49.9	50.0	51.8	50.6	51.1	51.6	49.9	52.2
Al ₂ O ₃	0.04	0.03	0.06	0.08	0.02	0.02	0.04	0.05	0.03	0.06	0.08	0.07	0.04	0.02	0.03	0.03	0.01	0.10	0.04	0.04
Cr ₂ O ₃	0.08	0.09	0.05	0.07	0.05	0.05	0.05	0.07	0.07	0.14	0.08	0.12	0.08	0.05	0.03	0.06	0.07	0.08	-	-
FeO ^c	46.5	45.2	45.2	44.0	42.9	43.1	43.1	40.8	40.6	43.6	43.3	42.8	47.7	47.1	45.1	45.3	44.2	41.5	47.7	41.8
MnO	2.86	2.98	2.99	4.22	5.07	4.41	4.48	6.95	7.01	3.65	3.76	4.08	1.04	2.05	3.21	4.09	4.72	5.56	1.48	4.34
MgO	0.04	0.04	0.05	0.04	0.05	0.07	0.03	0.01	0.02	0.20	0.11	0.12	0.11	0.08	0.05	0.07	0.05	0.07	0.19	0.18
CaO	-	0.02	0.17	0.22	0.04	0.01	0.03	0.06	0.15	0.04	0.07	0.18	0.12	0.02	0.01	0.04	0.02	0.33	0.12	0.03
Total	99.7	99.2	100.4	99.9	99.1	99.8	99.9	98.9	99.4	99.6	99.8	99.5	99.1	99.3	100.3	100.3	100.2	99.5	99.6	98.7
Calculated normative components																				
MnTiO ₃	6.09	6.34	6.36	8.98	10.8	9.39	9.53	14.8	14.9	7.77	7.99	8.69	2.21	4.35	6.83	8.69	10.0	11.8	3.14	9.23
FeTiO ₃	88.9	89.8	91.8	88.0	85.7	89.3	89.2	81.6	82.4	90.0	91.1	89.7	92.1	90.3	91.3	87.1	86.9	85.8	91.0	89.2
Fe ₂ O ₃	4.90	2.98	1.93	2.63	2.62	0.90	0.95	2.46	1.74	1.06	0.19	0.39	4.49	4.80	2.05	4.54	3.37	0.93	5.19	-
MgTiO ₃	0.11	0.12	0.15	0.11	0.15	0.21	0.10	0.02	0.05	0.60	0.33	0.37	0.32	0.25	0.16	0.22	0.14	0.21	0.57	0.54
Total R ₂ O ₃	100.1	99.4	100.4	99.9	99.3	99.9	99.9	99.0	99.2	99.6	99.8	99.1	99.2	99.8	100.4	100.6	100.5	98.9	99.9	99.0

No. ^a	36-2-8	37-1-2	37-2-3	37-2-4	38-1-1	38-1-2	39-1-5	39-1-6	40-1-3	40-1-4	42-1-6	42-2-1	43-1-1	43-2-2	43-3-3	45-1-5	45-1-6	46-1-1	46-1-2	46-2-4
Occurrence ^b	P-I-R	P-I-R	P-I-C	P-I-R	P-I-C	P-I-R	P-I-C	P-I-R	P-I-C	P-I-R	P-I-C	P-C1	G-I-C	G-I-C	G-L	P-I-C	P-I-R	P-I-C	P-I-R	P-C1
SiO ₂	0.12	0.11	0.15	0.10	0.05	0.03	0.01	-	0.11	0.08	0.01	0.04	0.18	0.20	0.10	0.01	0.03	0.07	0.04	0.01
TiO ₂	51.5	52.0	52.2	52.2	49.5	50.1	49.9	50.6	49.6	50.0	48.9	48.3	48.3	47.8	48.8	47.5	47.4	46.6	46.7	45.7
Al ₂ O ₃	0.04	0.04	0.06	0.05	0.03	0.02	0.03	0.03	0.03	0.03	0.07	0.03	0.07	0.06	0.06	0.04	0.05	0.04	0.04	0.06
Cr ₂ O ₃	-	0.10	0.09	0.09	0.05	0.05	0.03	0.06	0.10	0.06	0.04	0.04	0.08	0.05	0.08	0.07	0.06	0.05	0.06	0.09
FeO ^c	44.4	44.1	43.2	43.2	47.2	47.0	46.0	45.4	45.4	45.0	44.5	41.9	45.2	44.9	42.9	45.1	44.9	43.0	43.5	42.5
MnO	4.35	3.11	3.54	3.67	2.30	2.41	3.28	3.71	3.84	4.12	5.41	8.48	4.77	5.70	6.82	5.48	5.56	8.10	8.29	9.68
MgO	0.18	0.10	0.16	0.15	0.03	0.04	0.03	0.03	0.04	0.04	0.15	0.27	0.06	0.07	0.04	0.10	0.09	0.20	0.21	0.12
CaO	0.04	0.11	0.07	0.11	0.03	0.03	0.01	0.07	-	0.16	0.06	0.04	0.11	0.11	0.13	0.06	0.08	0.06	0.05	-
Total	100.6	99.7	99.5	99.6	99.2	99.7	99.3	99.9	99.1	99.5	99.1	99.1	98.8	98.9	98.9	98.4	98.2	98.1	98.9	98.2
Calculated normative components																				
MnTiO ₃	9.26	6.62	7.53	7.80	4.89	5.12	6.97	7.89	8.17	8.76	11.5	18.0	10.1	12.1	14.5	11.7	11.7	17.2	17.6	20.6
FeTiO ₃	87.8	91.8	91.0	90.7	89.0	89.8	87.6	88.1	85.9	86.0	80.7	72.5	81.2	78.3	77.8	78.1	77.8	70.3	70.2	65.6
Fe ₂ O ₃	3.13	0.72	0.13	0.26	5.67	5.03	4.97	4.11	5.31	4.71	6.99	8.37	7.48	8.69	6.73	9.03	8.97	10.7	11.4	12.7
MgTiO ₃	0.54	0.28	0.47	0.45	0.08	0.11	0.09	0.07	0.12	0.11	0.45	0.81	0.18	0.20	0.13	0.30	0.26	0.60	0.62	0.34
Total R ₂ O ₃	100.8	99.6	99.3	99.4	99.7	100.1	99.7	100.3	99.6	99.7	99.8	99.8	99.1	99.4	99.3	99.2	98.9	98.9	99.9	99.4

No. ^a	46-2-1	46-2-2	46-2-5	47-1-1	47-1-2	47-2-3	48-1-1	48-2-2	49-1-3	49-1-4	49-2-7	50-1-3	50-1-4	50-2-5	50-3-6	50-4-7	51-1-1	51-1-2	51-2-3	51-2-4
Occurrence ^b	P-L	P-L	P-C2	P-I-C	P-I-R	G-I-C	P-I-C	P-I-C	P-I-C	P-I-R	P-C1	P-I-C	P-I-R	P-I-R	G-I-C	G-I-C	P-I-C	P-I-R	P-I-C	P-I-R
SiO ₂	0.03	0.03	0.01	0.07	0.13	0.20	0.07	0.07	0.09	0.08	0.09	0.07	0.05	0.04	0.08	0.07	0.14	0.04	0.14	0.13
TiO ₂	45.5	45.7	46.4	47.2	46.7	46.8	48.8	50.3	45.9	45.7	47.7	48.7	48.7	49.4	48.9	48.7	47.6	47.5	47.2	46.8
Al ₂ O ₃	0.06	0.05	0.05	0.21	0.22	0.17	0.24	0.18	0.07	0.05	0.04	0.10	0.05	0.08	0.05	0.10	0.04	0.03	0.05	0.04
Cr ₂ O ₃	0.07	0.08	0.07	0.08	0.08	0.10	0.09	0.08	0.03	0.04	0.03	0.04	0.05	0.05	0.05	0.05	0.10	0.06	0.08	0.05
FeO ^c	42.5	41.5	40.1	47.2	46.3	45.6	44.5	43.5	45.2	44.3	42.2	44.2	43.2	42.4	41.3	40.5	43.4	42.8	41.0	40.1
MnO	9.86	10.5	12.1	3.14	4.82	5.82	5.49	5.94	7.51	7.68	8.89	7.14	7.94	8.14	9.18	9.98	7.97	8.12	9.91	10.9
MgO	0.09	0.08	0.04	1.43	0.41	0.08	0.21	0.22	0.08	0.10	0.03	0.08	0.07	0.09	0.08	0.08	0.03	0.01	0.06	0.04
CaO	-	-	-	0.02	0.08	0.15	0.15	0.13	0.02	0.09	0.06	0.03	0.03	0.02	0.06	0.12	0.02	0.03	0.02	0.08
Total	98.1	98.0	98.8	99.4	98.7	98.9	99.6	100.4	98.9	98.0	99.0	100.4	100.1	100.2	99.7	99.6	99.3	98.6	98.5	98.2
Calculated normative components																				
MnTiO ₃	21.0	22.5	25.7	6.67	10.3	12.4	11.7	12.6	16.0	16.3	18.9	15.2	16.9	17.3	19.5	21.2	16.9	17.3	21.1	23.3
FeTiO ₃	65.0	63.7	62.1	77.5	76.9	76.0	80.1	81.9	70.7	70.1	71.4	76.9	75.2	76.1	72.9	70.9	73.3	72.8	68.1	65.4
Fe ₂ O ₃	13.0	12.6	11.8	11.7	11.0	10.6	7.30	5.29	13.0	12.4	9.40	8.67	8.48	7.09	7.57	7.67	9.61	9.31	9.67	10.1
MgTiO ₃	0.27	0.25	0.12	4.28	1.23	0.25	0.61	0.66	0.23	0.30	0.09	0.23	0.21	0.26	0.25	0.23	0.09	0.04	0.17	0.11
Total R ₂ O ₃	99.4	99.3	99.8	100.4	99.7	99.5	100.0	100.7	100.0	99.2	99.9	101.1	100.9	100.9	100.3	100.2	100.0	99.5	99.2	99.0

^a The two numbers following the specimen number refer to grain number and spot number. Specimen numbers correspond to those of Table 2.

^b First letter indicates whether crystal occurs as phenocryst phase (P) or groundmass phase (G). Second letter indicates whether crystal is independent grain type (I), trellis type (L), external granule type (C₁) or internal granule type (C₂). Third letter indicates whether analysis of core (C) or rim (R).

^c Total Fe as FeO

Analysts: T. Imaoka (Nos. 5, 16-21, 23, 24, 27, 29-32, 37, 40, 42, 48-51) and K. Nakashima (others).

are: 15 kv accelerating voltage, about 0.02 μ A specimen current. Five countages of 10 seconds integration time were averaged for a single complete analysis. Analyses were made for elements Si, Ti, Al, Cr, Fe, Mn and Ca on the polished thin sections coated with carbon simultaneously with standards set in the brass plate, using natural and synthetic oxides as the standard. Raw data

were corrected by the method of Bence and Albee (1968) using alpha-factors of Nakamura and Kushiro (1970).

The amounts of Fe_2O_3 and FeO in magnetite were calculated from stoichiometric consideration using the procedures outlined by Carmichael (1967). "Normative" MnTiO_3 , FeTiO_3 , Fe_2O_3 and MgTiO_3 components for ilmenites were calculated

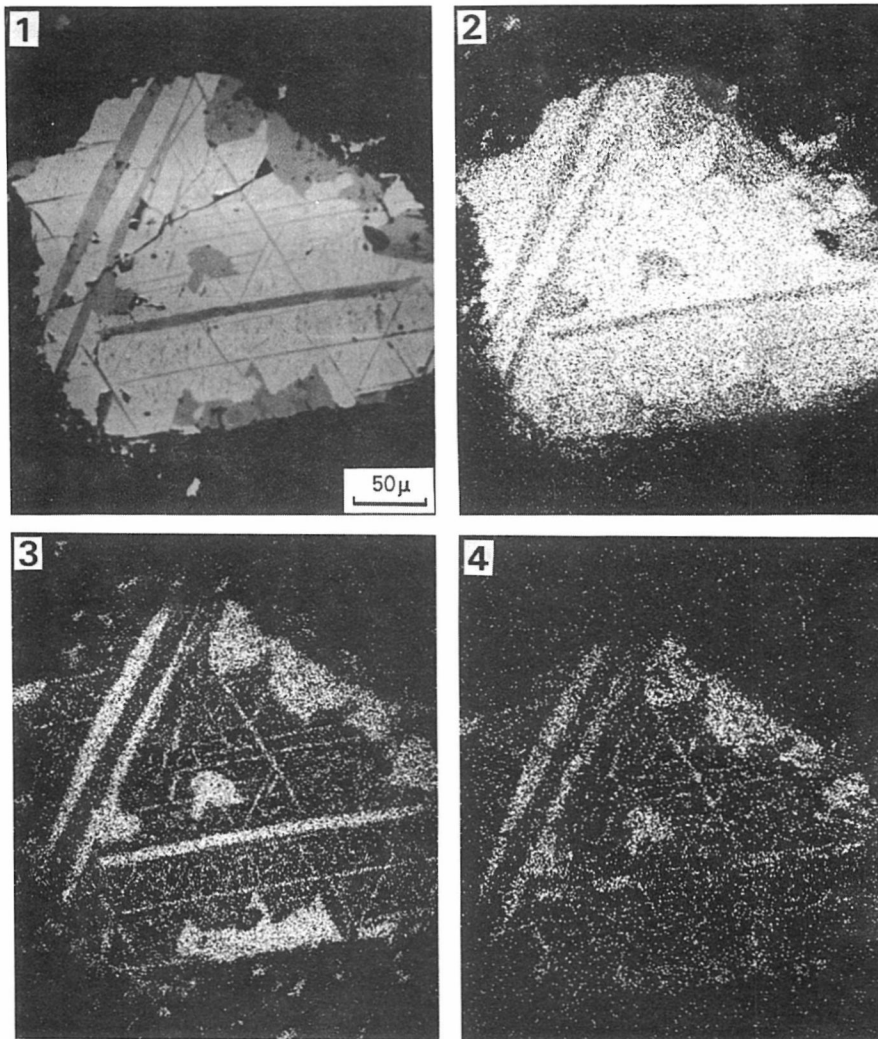


Fig. 3. Scanned images of analyzed magnetite phenocryst in andesite lava (Sp. no. 46) from the Paleogene Haza cauldron.

no. 1: Secondary electron beam image, no. 2: characteristic X-ray image (Fe $K\alpha$), no. 3: ditto (Ti $K\alpha$), no. 4: ditto (Mn $K\alpha$).

according to the method proposed by Anderson (1968).

An electron beam of approximately 2–3 μm diameter was used usually to analyse oxides, but bulk analyses of magnetite with ilmenite lamellae were made with a beam of about 30 μm diameter on many points of several grains and were averaged.

1. Chemistry of ilmenite

From the above description of the occurrence, the ilmenites are divided into four types according to the Buddington and Lindsley (1964) classification:

- (a) independent (single) grain type
- (b) trellis type
- (c) composite (granular) type
 - (c₁) internal granule type
 - (c₂) external granule type

To investigate the compositional relationships among these four types of ilmenite, specimen no. 46 (clinopyroxene andesite lava from Haza cauldron, Tamagawa Group) was especially selected, because of its least alteration and containing all four types of ilmenite. As illustrated in Figs. 3 and 4, the phenocrystic magnetite has well-developed ilmenite lamellae parallel to its (111) plane together with finer sets of ilmenite lamellae of several generations. Moreover, ilmenites of composite type (both internal and external) are also observed.

The analytical result of four types of ilmenite is shown in Table 3 (no. 46) and

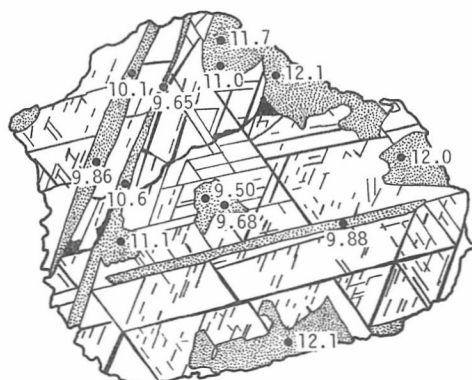


Fig. 4. Variation of MnO content of ilmenites depending on their mode of occurrences in specimen no. 46.

Fig. 4. As is clear from these data, there is a significant difference in the MnO content of ilmenite among four types. That is, the MnO content increases in the following order; independent grain type (8.10–8.29%), internal granule type (9.50–9.68%), trellis type (9.65–10.6%) and external granule type (11.0–12.1%). The MnO content of internal granule along the cavity (11.1%) is as high as that of external granule.

In many cases, the examined ilmenites of independent grain type show various degrees of zoning with usual increase of MnO or pyrophanite (MnTiO_3) molecules from core to rim (Table 3). However, in the ilmenite from the Hikimi volcanic rocks, this variation of Mn is slight or nearly constant accompanied by decrease of hema-

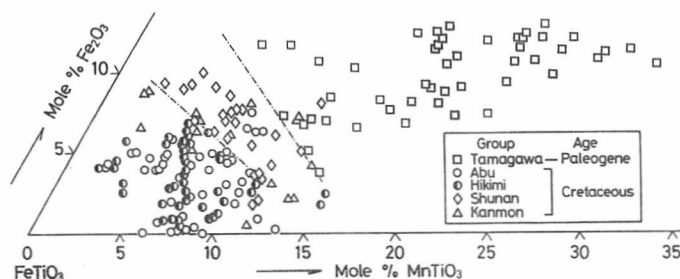


Fig. 5. FeTiO_3 - Fe_2O_3 - MnTiO_3 diagram for ilmenites in volcanic rocks.

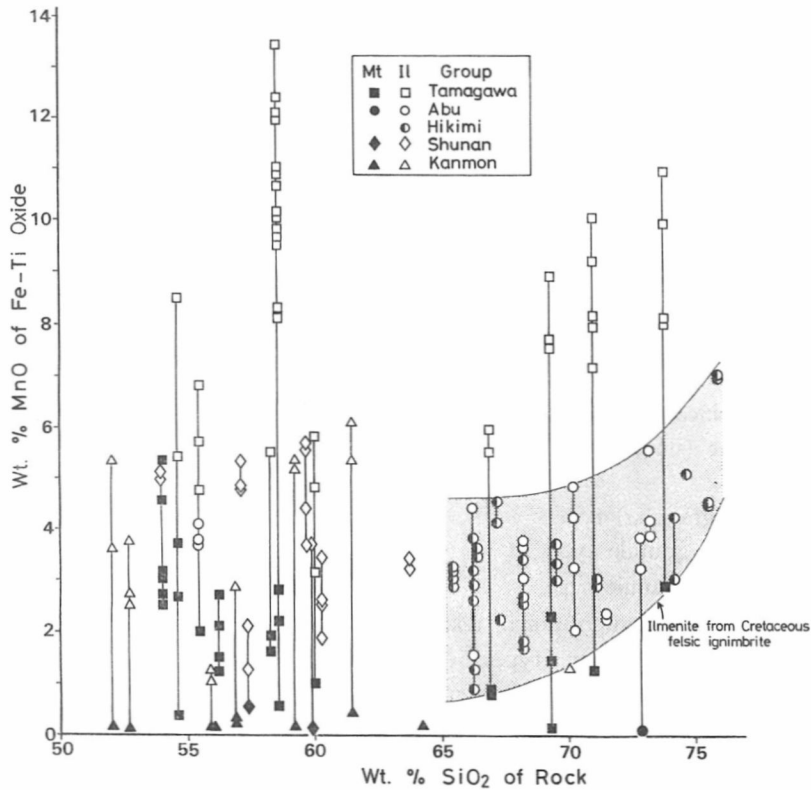


Fig. 6. SiO_2 wt. percent of whole rock vs. MnO content of ilmenite and coexisting magnetite.

tite (Fe_2O_3) molecules toward rim. In addition, the MnO content of ilmenite is larger in the groundmass phase than in the phenocrystic one (Table 3, e.g., nos. 34, 47 and 50).

As for the chemical composition of ilmenite, there is a difference among four textural types and among five groups of volcanic rocks. The latter difference is far larger than the former as illustrated in Fig. 5. That is, ilmenites from the Kanmon, Hikimi and Abu Groups are poorer in MnTiO_3 (1.9–14.9 mol.%) and also in Fe_2O_3 (0.9–8.3 mol.%) than those from the Tamagawa Group (6.7–28.5 mol. % in MnTiO_3 and 5.3–13.0 mol. % in Fe_2O_3). Ilmenite from the Shunan Group is in intermediate between

the above-cited two groups of composition.

Fig. 6 shows the relationship between the SiO_2 content of whole rock and the MnO content of ilmenite and magnetite. From this diagram, it is clear that there is a difference in the MnO content of ilmenite between Mesozoic and Paleogene volcanic rocks, even when the rocks have the same basicity. Moreover, the manganese is preferentially concentrated in ilmenite, comparing with the coexisting magnetite (Figs. 3 and 6).

2. Chemistry of magnetite

As described before, magnetite constitute the major oxide phase in the volcanic rocks belonging to the magnetite-series (Ishihara, 1977) such as in those from the

Table 4. Averaged microprobe analyses of magnetites

Sp. No. ^a	1	2	3	4	4	5	6	7	8	11	16	39	41
Occurrence ^b	Gm	Ph	Ph	Ph	Gm	Ph	Gm	Gm	Ph	Ph	Gm	Ph	Ph
SiO ₂	0.29	0.16	0.24	2.35	2.74	0.39	0.96	0.69	0.84	0.07	0.48	0.17	0.21
TiO ₂	0.05	0.14	20.8	13.7	23.4	0.65	0.37	11.7	2.09	12.3	0.51	0.98	12.9
Al ₂ O ₃	-	0.14	0.40	0.70	0.35	0.46	0.39	0.28	0.14	2.06	0.08	0.08	2.78
Cr ₂ O ₃	0.59	0.11	0.39	0.20	0.07	1.13	0.89	0.19	0.16	0.38	0.21	0.10	0.12
FeO ^c	91.6	92.4	75.1	78.6	69.0	89.2	89.3	80.6	89.4	78.9	91.1	90.9	77.6
MnO	0.16	0.13	0.15	0.15	0.15	0.26	0.16	0.42	0.18	0.55	0.14	0.10	2.84
MgO	0.04	0.03	0.33	0.13	0.33	0.03	0.15	0.03	0.07	0.06	0.02	0.02	0.12
CaO	0.17	0.02	0.12	0.29	0.42	0.14	0.19	0.05	0.09	0.12	0.07	0.04	0.03
Total	92.9	93.1	97.5	96.1	96.5	92.3	92.4	94.0	93.0	94.4	92.6	92.4	96.6
Recalculated analyses													
Fe ₂ O ₃	67.4	68.0	27.8	35.9	15.8	64.3	63.9	43.1	62.2	41.3	66.0	65.8	40.9
FeO	30.9	31.2	50.1	46.3	54.8	31.3	31.8	41.8	33.5	41.7	31.7	31.7	40.9
Total	99.6	99.9	100.3	99.7	98.1	98.7	98.8	98.3	99.3	98.5	99.2	99.0	100.8
Mol. % Usp.	1.28	1.00	59.4	47.4	76.7	3.44	4.77	36.6	9.29	35.5	3.34	3.51	36.7

Sp. No. ^a	41	41	42	43	44	44	45	46	47	48	49	50	51
Occurrence ^b	Mp	Gm	Ph	Ph	Ph	Gm	Ph	Ph	Ph	Ph	Ph	Gm	Ph
SiO ₂	0.45	0.64	0.08	0.20	0.17	0.40	0.27	0.14	0.29	0.10	0.23	0.18	0.14
TiO ₂	18.4	19.6	10.7	16.0	6.93	21.5	14.0	10.3	13.3	5.93	8.98	8.99	12.9
Al ₂ O ₃	1.47	1.09	0.65	0.48	3.76	0.11	1.45	0.93	2.25	1.86	2.94	2.32	1.40
Cr ₂ O ₃	0.13	0.09	0.07	0.19	7.87	0.08	0.15	0.06	0.24	0.09	0.05	0.10	0.07
FeO ^c	71.3	69.7	81.2	76.1	74.6	71.8	77.1	80.2	76.2	83.5	80.8	81.4	78.8
MnO	4.74	5.23	2.24	1.98	1.36	2.39	1.77	2.19	2.55	0.84	1.30	1.26	2.87
MgO	0.04	0.04	0.10	0.06	0.08	0.14	0.06	0.08	0.18	1.07	0.10	0.06	0.05
CaO	0.07	0.13	0.08	0.08	0.04	0.19	0.12	0.08	0.12	0.03	0.05	0.04	0.01
Total	96.6	96.5	95.1	95.1	94.8	96.6	94.9	94.0	95.1	93.4	94.5	94.4	96.2
Recalculated analyses													
Fe ₂ O ₃	30.4	27.9	47.4	36.1	42.1	25.9	38.7	46.8	39.2	54.9	47.0	47.8	42.4
FeO	44.0	44.6	38.6	43.6	36.7	48.4	42.3	38.1	40.9	34.2	38.5	38.4	40.7
Total	99.7	99.3	99.9	98.7	99.0	99.1	98.8	98.7	99.0	99.0	99.2	99.2	100.5
Mol % Usp.	53.6	58.0	30.7	46.7	20.4	62.6	41.1	30.3	38.8	17.3	26.3	26.4	37.0

^a Specimen numbers correspond to those of Table 2.

^b Ph=phenocryst, Mp=microphenocryst, Gm=microcryst in groundmass.

^c Total Fe as FeO

Analysis: T. Imaoka (Nos. 4, 5, 16, 41, 42, 44, 48-51) and K. Nakashima (others).

Kanmon and Tamagawa Groups. Some specimens from the Shunan and Abu Groups also contain magnetite. Their analytical data are listed in Table 4.

The chemical composition of magnetite varies with its mode of occurrence. In the ilmenite-free specimens (nos. 41 and 45), three types of magnetite are discerned in its generation; phenocryst, micro-phenocryst, and microcryst in the groundmass. The former two types show the evidence of magmatic corrosion, while the third is euhedral. This may mean an earlier stage of crystallization of the former two than the third type.

As is clear from Table 4 (nos. 41 and 44), there is a marked increase of Ti, a slight increase of Mn and a decrease tendency of total Fe, Al, and Mg in the following order; phenocryst, microphenocryst, groundmass.

Similar trends are known also in some basalts and andesites (Oshima, 1971; Anderson and Wright, 1972; Prevot and Mergoill, 1973). As stated by Oshima (1971, 1975), the increase of ulvöspinel molecules as crystallization proceeds can be attributed to the decrease of temperature on the liquidus surface in the spinel field in the FeO-Fe₂O₃-TiO₂ system (Taylor, 1963), and this is related to the increase of liquidus and solidus

temperatures associated with the decrease of vapor pressure while the eruption takes place. The decrease of the Al and Mg contents in magnetite is associated with the increase of ulvöspinel molecule (Carmichael and Nicholls, 1967; Oshima, 1971; Prévot and Mergoil, 1973). This is attributable to the decrease of temperature (Oshima, 1975). The increase of the Mn content is probably correlated with the progressive differentiation of the residual magma (Prévot and Mergoil, 1973). Comparing with ilmenite, the MnO content of magnetite is not so conspicuous excepting the magnetite from ilmenite-free volcanic rocks (no. 41, containing up to 5.35% MnO). This is due to the selective partition of Al, Cr in magnetite and Mn in ilmenite during the progressive crystallization of magma as reported by many authors. Trace amount of Ni is present in magnetite from the Kanmon Group, but not in ilmenite.

Discussion and conclusion

The above description indicates the fairly different chemical composition of

ilmenite among five volcanic groups. That is, the ilmenite from the Paleogene Tama-gawa volcanic rocks is richer in pyrophanite and hematite molecules than those from the Cretaceous volcanic rocks (e.g., the Kanmon, Shunan, Hikimi and Abu Groups). This chemical difference of ilmenite is observed also between Cretaceous granitic rocks and Paleogene ones. This was verified by Imaoka *et al.* (1979) between Paleogene granitoids and Cretaceous granitoids from the San'yo and Ryoke Zones (Fig. 7). What is the difference attributable to?

Generally, the Mn^{2+}/Fe^{2+} ratio of ilmenite and the partition relation of Mn between coexisting ilmenite and magnetite essentially depend on:

- 1) Temperature of crystallization (Buddington and Lindsley, 1964; Anderson, 1968; Dasgupta, 1970; Duchense, 1972; Neumann, 1974).
- 2) Mn/Fe ratio in the magma from which the oxides crystallized (Tsusue, 1973; Neumann, 1974).
- 3) Oxygen fugacity (Anderson, 1968; Czamanske and Mihálik, 1972; Neumann,

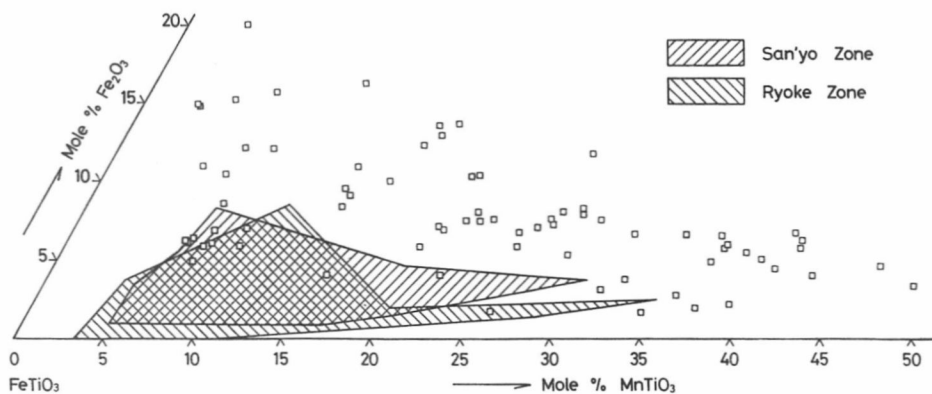


Fig. 7. $FeTiO_3$ - Fe_2O_3 - $MnTiO_3$ plots for ilmenites from Paleogene granitic rocks in the Inner Zone of Southwest Japan.

Compositional ranges of ilmenites from Cretaceous granitoids of Ryoke and San'yo zones are illustrated by shadowed portions. Data from Tsusue and Ishihara (1974), Tainosho *et al.* (1979), Czamanske *et al.* (1981) and this study.

1974).

The $Mn_{Il}^{2+}/Mn_{Mt}^{2+}$ and $(Mn^{2+}/Fe^{2+})_{Il}$ ratio will increase more strongly with increasing $(Mn^{2+}/Fe^{2+})_{magma}$ at low temperatures than at high temperatures. At a given temperature and isochemical condition, the $Mn_{Il}^{2+}/Mn_{Mt}^{2+}$ and Mn^{2+}/Fe^{2+} ratio of ilmenite will increase with increasing oxygen fugacity, whereas the $Mn_{Il}^{3+}/Mn_{Mt}^{3+}$ ratio will decrease.

Some discussions on the three controll-

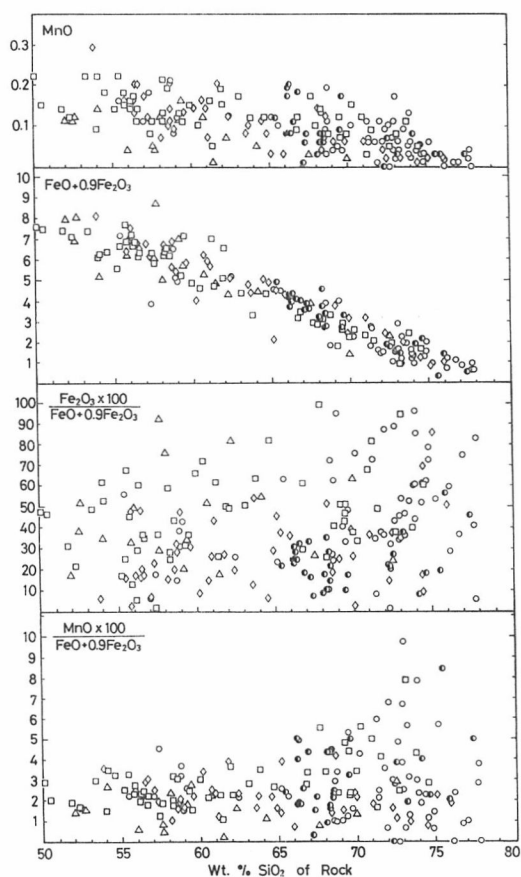


Fig. 8. Variation diagram for volcanic rocks in respect to MnO, $FeO+0.9Fe_2O_3$, $Fe_2O_3 \times 100 / (FeO + 0.9Fe_2O_3)$ and $MnO / (FeO + 0.9Fe_2O_3)$ ratio.

Data from Imaoka & Murakami (1979), Murakami & Imaoka (1980) and this study. Symbols are same as in Fig. 2.

ing factors will be given below. The evolutionary trends and the structural state of alkali-feldspar (Murakami, 1974, 1977) and the temperature calculated by using two-feldspar geothermometer (Tainosho *et al.*, 1979) indicate that the Paleogene granitoids from the San'in Zone have been crystallized at a higher temperature than the Cretaceous granitoids from the San'yo and Ryoke Zones. This is inconsistent with the fact of Mn-enrichment of ilmenite from the San'in Zone.

Tsuse (1973) showed that there is a direct positive relation in the MnO/FeO ratio between ilmenites and their host rocks in his investigation on the four granites from the Osumi Peninsula, South Kyushu, Japan. Although there is no great difference in the MnO content of these rocks, the MnO/FeO ratio of these host rocks increases with the differentiation index. This means the effect of whole rock chemistry.

Fig. 8 shows the variation of MnO, $FeO+0.9Fe_2O_3$, $Fe_2O_3 \times 100 / (FeO + 0.9Fe_2O_3)$ ratio and $MnO / (FeO + 0.9Fe_2O_3)$ ratio in respect to the SiO_2 content of volcanic rocks. As indicated in this figure, no discernible difference is observed on MnO, $FeO+0.9Fe_2O_3$ and $MnO / (FeO + 0.9Fe_2O_3)$ ratio at given SiO_2 percent among five volcanic formations, although the $Fe_2O_3 \times 100 / (FeO + 0.9Fe_2O_3)$ ratio is distinctly lower in the Hikimi volcanic rocks than in the Tamagawa ones.

As for the plutonic rocks, too, there cannot be found any discernible difference in the Mn content between Paleogene and Cretaceous plutonic rocks despite of the difference in the Fe^{3+}/Fe^{2+} ratio (Ishihara, 1971; Murakami, 1974).

Neumann (1974) concluded that Mn^{2+} fits better into ilmenite structure than into magnetite structure, while Mn^{3+} probably

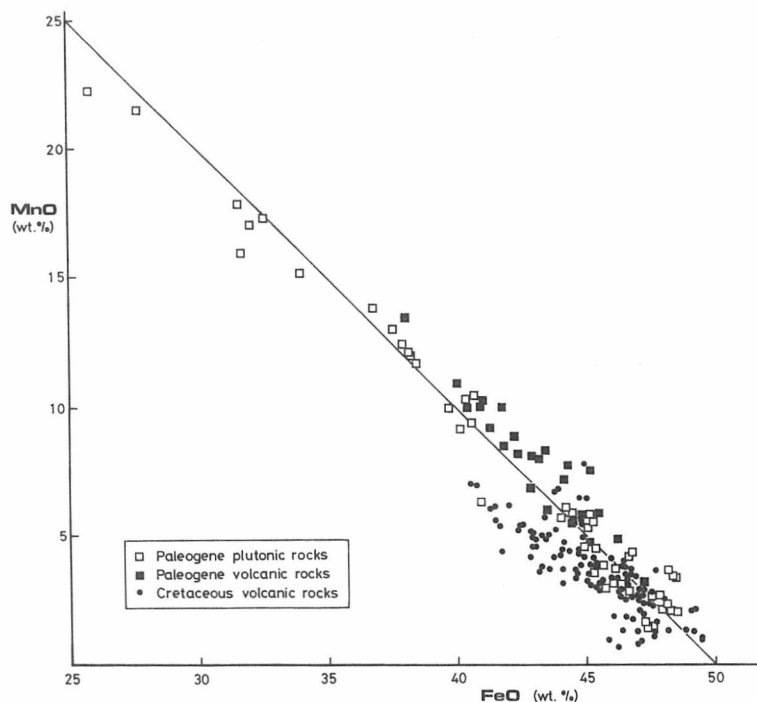


Fig. 9. MnO vs. total FeO for ilmenites.

fits better into magnetite structure than into ilmenite structure. The analyzed ilmenites in this work show a clear negative relationship between total MnO and total FeO (Fig. 9). As stated before, they are often strongly enriched in Mn compared with coexisting magnetites. This is consistent with the data so far reported (e.g., Buddington and Lindsley, 1964; Czamanske and Mihálik, 1972). In addition to these facts, Mn in these ilmenites satisfies their structural formula when Mn is calculated as Mn^{2+} . Judging from the above facts, most of Mn in the ilmenites examined is interpreted to be Mn^{2+} .

From the above discussion, we consider that the increase of the $MnTiO_3/FeTiO_3$ ratio in ilmenites in a suite of rocks is led by the increase of oxygen fugacity (Czamanske and Mihálik, 1972) as a result of preferred

oxidation of Fe^{2+} compared with Mn^{2+} , because of 10% lower ionization potential for Fe^{2+} to Fe^{3+} than for Mn^{2+} to Mn^{3+} (Orgel, 1960). Consequently, the strong Mn-enrichment in ilmenite from the Paleogene volcanic and plutonic rocks might have been caused by higher oxygen fugacity than the Cretaceous ones.

In volcano-plutonic association, it is worthy of note that the compositional range of ilmenite in plutonic rocks is far wider toward the pyrophanite end member than in volcanic rocks when Figs. 5 and 7 of the same age are compared. That is, the pyrophanite molecules of Cretaceous and Paleogene volcanic rocks range ca. 2–15% and ca. 7–29%, respectively, while those of plutonic rocks range ca. 4–35% and ca. 2–48%, respectively. This is probably because the plutonic rocks have a long slow

cooling history to consolidate and allow the constituent minerals to equilibrate at lower temperatures than the volcanic rocks.

Finally, we add that Czamanske *et al.* (1977) and Anderson (1980) showed a systematic partitioning of Mn between ilmenite and biotite, although it was not examined in this paper and at present the quantitative estimation of f_{O_2} and T of Fe-Ti oxides is not possible because MnTiO₃ cannot be ignored as an ilmenite component (Czamanske *et al.*, 1977). Experimental study to determine the effect of Mn on ilmenite-magnetite geothermometer-oxygen barometer such as in Mazzulo *et al.* (1975) will be expected.

References

- Anderson, A.T. (1968), Oxidation of the LaBlache Lake titaniferous magnetite deposit, Quebec. *J. Geol.*, **76**, 528-547.
- Anderson, A.T. and Wright, T.L. (1972), Phenocrysts and glass inclusions and their bearing on oxidation and mixing of basaltic magmas, Kilauea volcano, Hawaii. *Amer. Mineral.*, **57**, 188-216.
- Anderson, J.L. (1980), Mineral equilibria and crystallization conditions in the late Precambrian Wolf River rapakivi massif, Wisconsin. *Amer. J. Sci.*, **280**, 298-332.
- Bence, A.E. and Albee, A.L. (1968), Empirical correlation factors for the electron microanalysis of silicates and oxides. *J. Geol.*, **76**, 382-403.
- Buddington, A.F. and Lindsley, D.H. (1964), Iron-titanium oxide minerals and synthetic equivalents. *J. Petrol.*, **5**, 310-357.
- Carmichael, I.S.E. (1967), The iron-titanium oxide of salic volcanic rocks and their associated ferro-magnesian silicates. *Contrib. Mineral. Petrol.*, **14**, 36-64.
- Carmichael, I.S.E. and Nichols, J. (1967), Iron-titanium oxides and oxygen fugacity in volcanic rocks. *J. Geophys. Res.*, **72**, 4665-4687.
- Czamanske, G.K. and Mihalik, P. (1972), Oxidation during magmatic differentiation, Finmarka complex, Oslo area, Norway: Part 1, The opaque oxides. *J. Petrol.*, **13**, 493-509.
- Czamanske, G.K., Ishihara, S. and Atkin, S.A. (1981), Chemistry of rock-forming minerals of the Cretaceous-Paleogene batholith in Southwest Japan and implications for magma genesis. *J. Geophys. Res.*, **86**, 10431-10469.
- Czamanske, G.K., Wones, D.R. and Eichelberger, J.C. (1977), Mineralogy and petrology of the intrusive complex of the Pliny Range, New Hampshire. *Amer. J. Sci.*, **277**, 1073-1123.
- Dasgupta, H.C. (1970), Influence of temperature and oxygen fugacity on the fractionation of manganese between coexisting titaniferous magnetite and ilmenite. *J. Geol.*, **78**, 243-249.
- Duchense, J.-C. (1972), Iron-titanium oxide minerals in the Bjerkrem-Sogndal Massif, South-Western Norway. *J. Petrol.*, **13**, 57-81.
- Haggerty, S.E. (1976), Opaque mineral oxides in terrestrial igneous rocks. In *Oxide Minerals* (Rumble, D., III, Ed.). *Min. Soc. Am., Short Course Notes*, **3**, Hg-101-Hg-300.
- Hase, A. (1958), The stratigraphy and geologic structure of the late Mesozoic formations in western Chugoku and northern Kyushu. *Geol. Rep. Hiroshima Univ.*, **6**, 1-50 (in Japanese with English abstract).
- Imaoka, T. (1978), Petrological studies of the Paleogene Hamada cauldrons, Shimane Prefecture, Southwest Japan. *M. Sc. thesis, Hiroshima Univ.* (in Japanese with English abstract).
- Imaoka, T. and Nakashima, K. (in prep.), Magnetic susceptibility of Cretaceous to Neogene igneous rocks from the central and western Chugoku districts, Japan.
- Imaoka, T., Matsuhisa, Y. and Murakami, N. (1977), On the Kumogi granitic body, Shimane Prefecture, Southwest Japan — The possibility of meteoric ground water participation — *MAGMA*, No. 51, 8-14 (in Japanese).
- Imaoka, T. and Murakami, N. (1979), Petrochemistry of late Mesozoic to early Tertiary volcanic rocks in West Chugoku, Southwest Japan. *Mem. Geol. Soc. Japan*, No. 17, 259-272 (in Japanese with English abstract).
- Imaoka, T., Nakashima, K., Murakami, N. and Matsuda, T. (1979), The mode of occurrence and chemistry of Fe-Ti oxide minerals from Paleogene plutonic rocks in San-in Zone. *Program 1979 Joint Meet. Miner. Soc. Japan, Soc. Mining Geol., and Japan. Assoc. Min. Petr. Econ. Geol., Shizuoka*, 100 (in Japanese).
- Ishihara, S. (1971), Modal and chemical composition of the granitic rocks related to the major molybdenum and tungsten deposits in the inner zone of Southwest Japan. *J. Geol. Soc. Japan*, **77**, 441-452.
- Ishihara, S. (1977), The magnetite-series and

- ilmenite-series granitic rocks. *Mining. Geol.*, **27**, 293–305.
- Ishihara, S. (1979), Lateral variation of magnetic susceptibility of the Japanese granitoids. *J. Geol. Soc. Japan*, **85**, 509–523.
- Masuda Research Group (1982), Paleogene Masuda cauldrons. *J. Geol. Soc. Japan*, **88**, 321–335.
- Matsuda, T. (1976), Late Cretaceous to Paleogene volcanic rocks around Kawamoto-cho, Shimane Prefecture, central San-in district. *Abstr. Issue, 83th Annual Meet., Geol. Soc. Japan*, 235 (in Japanese).
- Matsuhisa, Y., Imaoka, T. and Murakami, N. (1980), Hydrothermal activity indicated by oxygen and hydrogen isotopes of rocks and minerals from a Paleogene cauldron, Southwest Japan. *Mining Geol., Spec. Issue*, No. 8, 49–65.
- Mazzullo, L.J., Dixon, S.A. and Lindsley, D.H. (1975), T- f_{O_2} relationships in Mn-bearing Fe-Ti oxides. *Abstr. Issue, Annual Meet., Geol. Soc. Amer.*, 1192.
- Murakami, N. (1973), A consideration on the mechanism of formation of the Paleogene Tamagawa cauldron, Southwest Japan. *Mem. Geol. Soc. Japan*, No. 9, 93–105 (in Japanese with English abstract).
- Murakami, N. (1974), Some problems concerning late Mesozoic to early Tertiary igneous activity on the inner side of Southwest Japan. *Pacific Geol.*, **8**, 139–151.
- Murakami, N. (1977), Compositional variation of some constituent minerals of the late Mesozoic to early Tertiary granitic rocks of Southwest Japan. *Geol. Soc. Malaysia, Bull.*, **9**, 75–85.
- Murakami, N. and Imaoka, T. (1980), Chemistry of late Mesozoic to Paleogene volcanic rocks in the Inner side of Southwest Japan with special reference to West Chugoku. *J. Japan. Assoc. Min. Petr. Econ. Geol., Spec. Issue*, No. 2, 263–278 (in Japanese with English abstract).
- Murakami, N. and Matsusato, H. (1970), Intrusive volcanic breccia in the late Mesozoic Zenjojima formation in western Chugoku and their possible relevance to the formation of cauldron structure. *J. Japan. Assoc. Min. Petr. Econ. Geol.*, **64**, 73–94.
- Murakami, N., Imaoka, T. and Izutsu, K. (1982), Geology and structure of Paleogene Haza cauldron, Shimane Prefecture, Southwest Japan. *J. Geol. Soc. Japan*, **88**, 311–319.
- Nakamura, E. (1979), On structure of volcanic depression, Paleogene Tertiary, Asahi-cho area, Shimane-ken, in the inner side of Southwest Japan. *Abstr. Issue, 86th Annual Meet., Geol. Soc. Japan*, 275 (in Japanese).
- Nakamura, Y. and Kushiro, I. (1970), Compositional relations of coexisting orthopyroxene, pigeonite and augite in a tholeiitic andesite from Hakone volcano. *Contrib. Mineral. Petrol.*, **26**, 265–275.
- Neumann, E.-R. (1974), The distribution of Mn^{2+} and Fe^{2+} between ilmenites and magnetites in igneous rocks. *Amer. J. Sci.*, **274**, 1074–1088.
- Orgel, L.E. (1960), Introduction to transition-metal chemistry: Ligandfield theory. pp. 186, Methuen, London.
- Oshima, O. (1971), Compositional variation of magnetite during the eruption and its bearing on the stage of crystallization of magma of Futatsu-dake, Haruna Volcano. *Mineral. J.*, **6**, 249–263.
- Oshima, O. (1975), Mineralogical aspects of volcanic eruption. *Bull. volcanol. Soc. Japan*, **20**, Spec. Number, 275–298 (in Japanese with English abstract).
- Prévoit, M. and Mergoil, J. (1973), Crystallization trend of titanomagnetites in an alkali basalt from Saint-Clément (Massif Central France). *Mineral. Mag.*, **39**, 474–481.
- Suzuki, M., Minami, A. and Yokoyama, S. (1977), Bulk chemical analysis of rocks by electron microprobe analyzer — with special reference to the direct fusion method. *Program 1977 Joint Meet. Miner. Soc. Japan, Soc. Mining Geol., and Japan. Assoc. Min. Petr. Econ. Geol., Niigata*, 41 (in Japanese).
- Taylor, R.W. (1963), Liquidus temperatures in the system $FeO-Fe_2O_3-TiO_2$. *J. Amer. Ceram. Soc.*, **46**, 276–279.
- Tainosho, Y., Honma, H. and Tazaki, K. (1979), Mineral chemistry in granitic rocks of East Chugoku, Southwest Japan. *Mem. Geol. Soc. Japan*, No. 17, 99–112.
- Tsuse, A. (1973), The distribution of manganese and iron between ilmenite and granitic magma in the Ōsumi peninsula, Japan. *Contrib. Mineral. Petrol.*, **40**, 305–314.
- Tsuse, A. and Ishihara, S. (1974), The iron-titanium oxides in the granitic rocks of Southwest Japan. *Mining Geol.*, **24**, 13–30 (in Japanese with English abstract).
- Williams, H. (1941), Calderas and their origin. *Univ. Calif. Publ. Dept. Geol. Sci.*, **25**, 239–346.
- Yoshida, H. (1961), The Late Mesozoic igneous activity in the middle Chugoku province. *Geol. Rep. Hiroshima Univ.*, **8**, 1–39 (in Japanese with English abstract).

西中国地域の白亜紀～古第三紀火山岩中の Fe-Ti 酸化鉱物
—とくにイルメナイト中の Mn 含有量について—

今岡 照喜・中島 和夫 (広島大・理)
村上 允英 (山口大・教養)

西中国地域の白亜紀～古第三紀火山岩中の Fe-Ti 酸化鉱物の産状及び化学組成について検討した。標題地域の火山岩層は下位より白亜紀の関門・周南・匹見・阿武層群及び古第三紀の田万川層群に区分される。このうち関門・田万川層群火山岩中には磁鉄鉱が卓越し、玄武岩質安山岩中よりクロムスピネルが見出された。一方、匹見・阿武層群火山岩中には磁鉄鉱はほとんど含まれない。周南層群火山岩中には、磁鉄鉱の卓越するものと全く欠くものの両者が共存する。全岩の帯磁率の測定結果も磁鉄鉱含有量の差をよく反映している。

イルメナイトは玄武岩質安山岩の一部を除くほとんど全ての火山岩中に含まれる。特にその Mn 含有量は産状により、また層群間で著しく変化する。すなわち、イルメナイトの産状は 1) independent type, 2) trellis type, 3) composite type に区分されるが、このうち同一薄片内では 1) より 2) 及び 3) に Mn が濃集している。また層群間でのイルメナイト中の Mn 含有量の差異は、これら産状による差異をはるかに凌駕しており、 $\text{FeTiO}_3\text{-Fe}_2\text{O}_3\text{-MnTiO}_3$ 図上で明瞭に識別できる。すなわち、古第三紀田万川層群火山岩中のイルメナイトは最も MnTiO_3 , Fe_2O_3 成分に富み、関門・匹見・阿武層群中のものは乏しい。周南層群中のものはその中間を示す。全体として白亜紀より古第三紀火山岩中のイルメナイトの方が MnTiO_3 , Fe_2O_3 成分に富む。深成岩中のイルメナイトについても同様の時代的差異が認められる。

イルメナイト中の Mn/Fe 比は温度・マグマ中の Mn/Fe 比, f_{O_2} などに支配されるが、古第三紀火山岩・深成岩における高 Mn/Fe 比は高い f_{O_2} に起因しているものと推定される。